Angulation Errors in Parallel-Hole and Fanbeam Collimators: Computer Controlled Quality Control and Acceptance Testing Procedure

Markus Eckholt and Helmar Bergmann

Department of Biomedical Engineering and Physics, University Hospital, Vienna; and Ludwig Boltzmann Institute of Nuclear Medicine, Vienna, Austria

Angulation errors in collimators of 1° or even less can seriously diminish the resolution of SPECT images. We have developed a computer-controlled quality control procedure that can be used for acceptance testing and regular routine checks. **Methods:** Using a marker point source and a computer-controlled x–y positioning table, we investigated 7 parallel-hole and 3 fanbeam collimators. The results are presented as collimator surface maps, which are easy to interpret visually. **Results:** The measurement accuracy for absolute angulation errors was better than 0.32°. Regional variations in channel tilt could be detected with an accuracy better than 0.16°. Six parallel-hole collimators were found acceptable for high-resolution SPECT imaging. For a parallel-hole collimator that had to be replaced because of nonoptimal image quality, our measurements clearly identified regions of directionally uniform angulation errors. Two fanbeam collimators showed slight concavities. **Conclusion:** Automation of the measurement and evaluation process make this procedure suitable for both acceptance tests and routine quality control checks. It can be applied to parallel-hole, fanbeam, converging, and diverging collimators, regardless of their individual geometry. No technical collimator specifications are needed. Our results reveal subtle mechanical deformations of collimators. They also show that for a detailed investigation, angulation error surface maps should be used to discover regional preferences in channel orientation.

Key Words: angulation; collimator; quality control; computer control

J Nucl Med 2000; 41:548–555

Collimators may show a wide range of defects resulting in low image quality, such as closed or imprecisely aligned channels and variations in channel diameter or septal thickness (*1,2*). Angulation errors of 1° or even less can seriously deteriorate the resolution of SPECT images (*1,3,4*). O'Connor (*5*) and Graham (*6*) have reported pertinent image examples. A comprehensive quality control assessment of a γ camera system must consequently investigate the current condition of a collimator.

Received Oct. 25, 1998; revision accepted Jul. 9, 1999.

For correspondence or reprints contact: Helmar Bergmann, MD, General Hospital Vienna, Deptartment of Biomedical Engineering and Physics, Waehringer Guertel 18–20, A-1090 Vienna, Austria.

In the work presented in this article, a quality control procedure for acceptance testing and regular routine checks has been developed. We confined ourselves to examining the alignment of collimator channels in parallel-hole and fanbeam collimators. To our knowledge, no related quality control procedure for fanbeam collimators has been introduced. The growing importance of fanbeam collimators in brain and cardiac studies (*5*) increases the need for such a procedure.

MATERIALS AND METHODS

The angulation of a collimator channel is defined as its actual angular orientation, and the angulation error of a channel is defined as the deviation in degrees from its nominal orientation (*1*). For the simple case of a parallel-hole collimator, the nominal orientation of all channels is perpendicular to the collimator face.

Measurement Principle

In the case of parallel-hole collimators, we place a radioactive point source at 2 distances D_c and D_r from the collimator face on 1 perpendicular line (Fig. 1). This produces a relative shift A between the point source images in the presence of an angulation error (Fig. 1B), in contrast to the case of correct channel orientation (Fig. 1A) (*1,7*). The limited spatial system resolution of a γ camera system does not allow direct measurement of the tilt of a single channel by this method (*1*). The measurement result is instead a local mean angulation value formed by a group of adjacent channels.

Because A has both x and y components, we represent the angulation error α as a vector. Its x component α_x is given by:

$$\alpha_x = \arctan\frac{A_x}{D} \approx \frac{A_x}{D}, \qquad \text{Eq. 1}$$

where $D = D_r - D_c$ is the height of a metal rod used to position the point source and A_x is the x component of A. For $\alpha_x < 4°$, the approximation introduces a relative error of less than 0.2%. The y component α_y is calculated analogously. For the total angulation error α, the equally good approximation is:

$$\alpha = \arctan\frac{A}{D} \approx \frac{A}{D} = \frac{\sqrt{A_x^2 + A_y^2}}{D} \approx \sqrt{\alpha_x^2 + \alpha_y^2}. \qquad \text{Eq. 2}$$

We image 2 identical grids of point source locations at both distances D_r and D_c to represent each angulation error result as a vector at the corresponding measurement location. This results in a surface map that is easy to interpret visually.

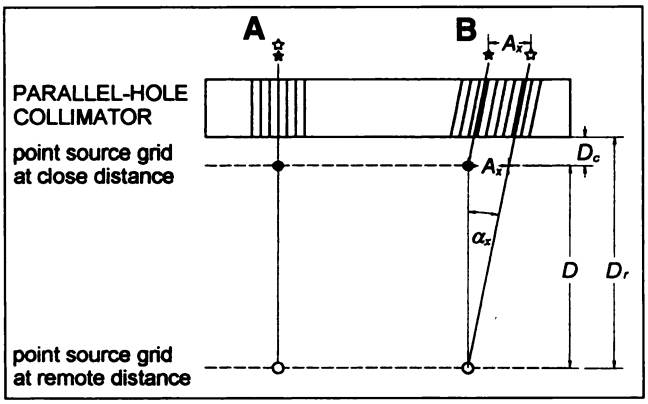

FIGURE 1. Measurement principle for parallel-hole collimators. Cross section of collimator along its x direction is presented. In contrast to correctly aligned channels (A), angulation error (B) produces relative shift between 2 point source images.

For fanbeam collimators, we modified the above measurement principle (Fig. 2). The following considerations and Equations 3–5 refer to the direction along the fan. It is perpendicular to the axis of rotation of the camera and is conventionally labeled the x direction in SPECT scans. To ensure that the 2 corresponding point source positions lie on the line given by the nominal orientation of the respective channel, the spacings g_c and g_r of the 2 grids cannot be identical. They must conform to the following equation:

$$\frac{g_r}{g_c} = \frac{m_c}{m_r}. \qquad \text{Eq. 3}$$

Here, m_c and m_r are image magnification factors of the fanbeam collimator. These factors are defined as the ratio of image size to object size and depend on the corresponding source-to-collimator distances D_c and D_r. The right side of the above equation is determined by measurement. One of the 2 arbitrarily programmable grid spacings may be chosen freely.

The angulation error formula is slightly more complex in the case of fanbeam collimators. According to Figure 2, $\xi = \arctan(X/D)$ is the nominal channel orientation. X is derived from the exactly known point source positions, and D already has been defined. We then have:

$$\tan(\xi + \alpha_x) = \frac{X + A_x}{D} = \tan\xi + \frac{A_x}{D}, \qquad \text{Eq. 4}$$

which yields:

$$\alpha_x = \arctan\left(\tan\xi + \frac{A_x}{D}\right) - \xi. \qquad \text{Eq. 5}$$

In the y direction parallel to the the axis of rotation, the channels of a fanbeam collimator are not tilted. For this direction, identical grid spacings for the close and the remote source-to-collimator distance must be chosen. The y component α_y of the angulation error is therefore calculated in analogy to Equation 1. The total angulation α is given by Equation 2.

Equations 3–5 can be applied without modification to converging and diverging collimators as well. The only difference is that the grid spacings must be matched for both the x and the y direction, and each component of the angulation error is calculated in analogy to Equation 5.

Technical Implementation

To position the point source with high accuracy and reproducibility, we constructed a computer-controlled step-motor–driven x–y

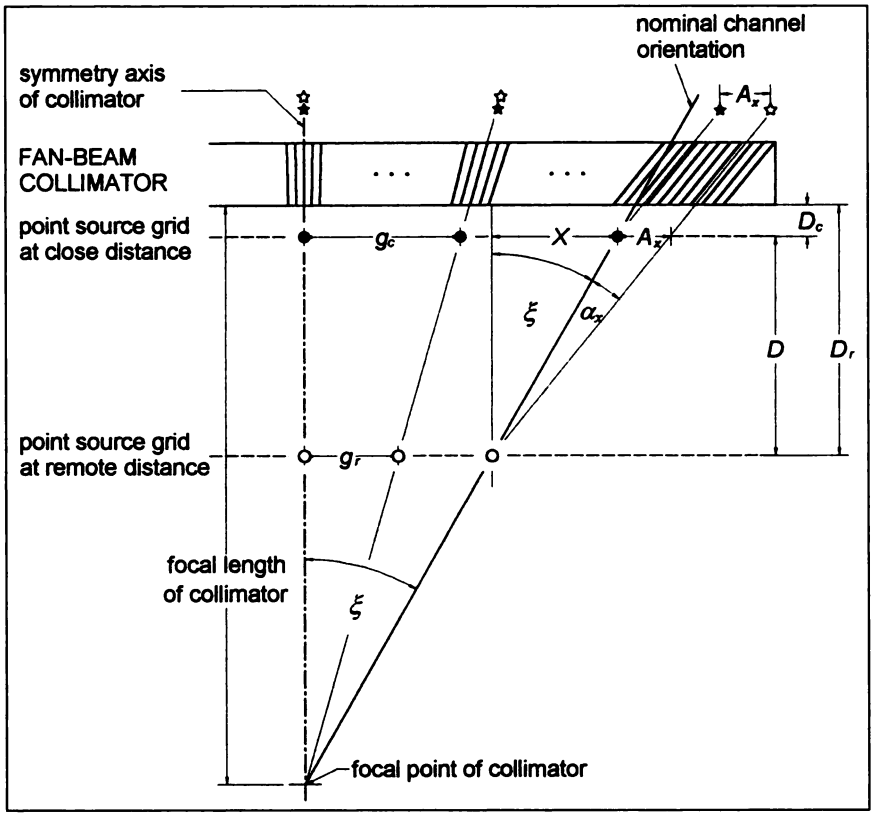

FIGURE 2. Measurement principle for fanbeam collimators. Cross section of collimator along fan (x direction) is shown. Grid spacings g_c and g_r are adapted to align source positions with nominal channel orientations. Angulation error causes shift between corresponding point source images.

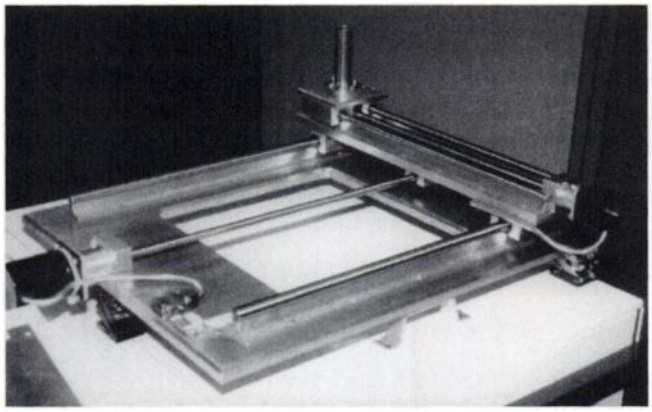

FIGURE 3. X–Y positioning table. Height of removable metal rod (upper right corner) is 10 cm. Rod can access any point within 37 × 41 cm^2 area.

positioning table made of aluminium (Fig. 3). The computer control consisted of a personal computer (486DX/40-MHz processor, 8-MB memory, 400-MB hard disk space) and a step-motor control unit (in-house manufacture). The mechanical reproducibility of positioning was determined to be <10 μm (maximum, 50 μm) and was therefore a negligible source of error. Before each measurement, both the x–y positioning table and the camera head were carefully adjusted horizontally with the aid of a level with an accuracy 0.5 mm/m (0.03°). The point sources used were a 3.7 MBq ^{57}Co marker source (Amersham Buchler Inc., Braunschweig, Germany) or ~2 μL ^{99m}Tc (3–6 MBq) in a hole in a small Lucite (Augmueller GmbH, Vienna, Austria) disk.

Parallel-Hole Collimators. For the first grid of measurement locations, the point source swept the collimator face at a distance of about D_c = 3 mm on top of the metal rod shown in Figure 3. For the second grid, we removed the rod and repeated exactly the same sweep with the point source in the remote position. This ensured a fixed distance of D = 10,000 ± 0.005 cm between the close and the remote point source position. We determined the x and the y component of the shift A for each grid point by calculation of the image centroids (*8*). For the creation of the angulation error surface maps, we used the software package MATLAB (The MathWorks, Inc., Natick, MA) on a personal computer to which the acquired images were transferred.

Fanbeam Collimators. In this case, the measurement procedure consisted of 2 parts. The first was identical to the complete measurement process for parallel-hole collimators (Fig. 4). This served to determine the exact position of the symmetry axis of the fan (the collimator center) and the ratio m_c/m_r used in Equation 3. For each grid row perpendicular to the symmetry axis of the collimator, the image centroid coordinates increased linearly with increasing distance of the corresponding point source positions from the symmetry axis. Figure 5 shows the straight lines resulting from linear regression, averaged over all grid rows. Their point of intersection represented the position of the collimator symmetry axis in grid coordinates, and the ratio of their slopes equaled the ratio m_c/m_r. In the second part of the procedure, the grid spacings were matched to fulfill Equation 3 (Fig. 2). The grid centers were made to coincide with the collimator center.

Collimator and Camera Specifications

We investigated 6 parallel-hole collimators in GCA-901-A single-head cameras (Toshiba Medical Inc., Vienna, Austria), 1 parallel-hole collimator in an APEX-SPX-6 single-head camera (Elscint Central & Eastern Europe, Vienna, Austria), and 3 fanbeam collimators in a Prism 3000 triple-head camera (Picker International Inc., Hofheim-Ballau, Germany). Technical specifications for these collimators are listed in Table 1. We chose the maximum digital matrix sizes available (1024 × 1024 pixels in the case of the Toshiba cameras and 512 × 512 pixels for both the Picker and Elscint cameras) and the recommended default energy window settings (20%, 15%, and 10%, respectively). A shift of the image centroid caused by a 1° angulation error would then be 3.5 pixels (Toshiba), 2.0 pixels (Picker), and 1.6 pixels (Elscint), with pixel sizes of 0.5, 0.9, and 1.1 mm, respectively.

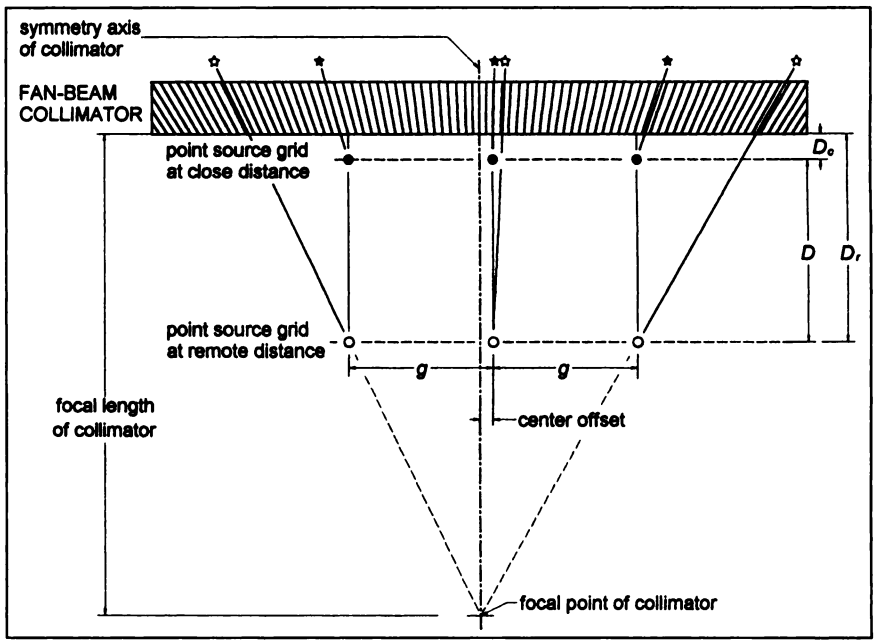

FIGURE 4. First part of measurement procedure for fanbeam collimators. Two identical point source grids (with grid spacing g) at different distances from collimator face are imaged. Relation between image positions and corresponding point source locations is linear (Fig. 5). Center of grids may be positioned freely with respect to center of collimator, which produces center offset (Table 3).

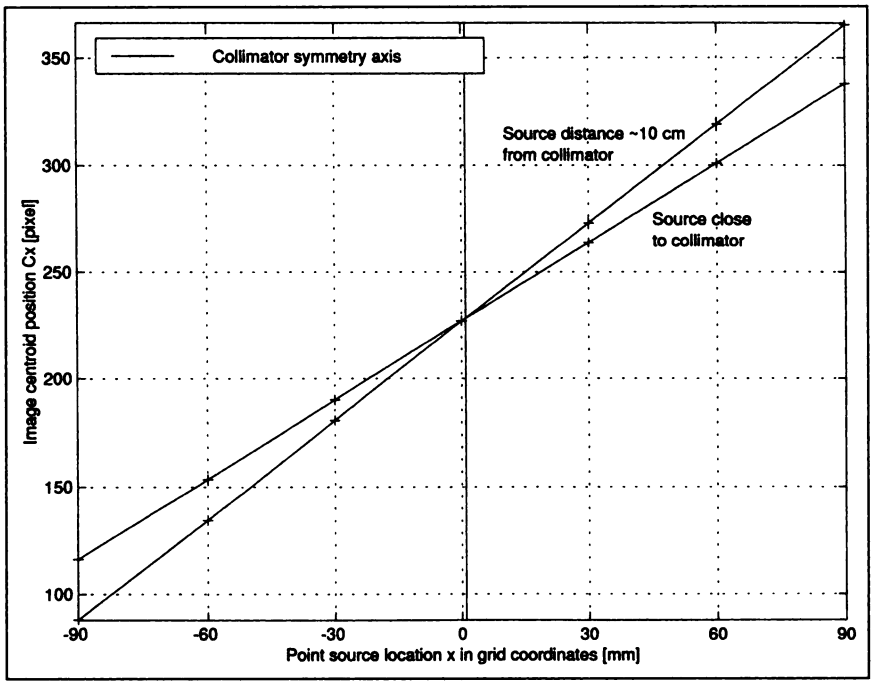

FIGURE 5. Results of first part of measurement procedure for fanbeam collimator RN1. Image centroid positions C_x averaged over all grid rows are plotted versus corresponding point source locations x, where x = 0 denotes center positions for both grids. Each source–collimator distance produces 1 line. Error bars are too small to be plotted (maximum SD was 0.8 pixel or 0.7 mm). Vertical line runs through point of intersection and indicates position of collimator symmetry axis.

RESULTS

Measurement Error of Determination of Angulation Error

For a parallel-hole collimator of a Toshiba single-head camera, 5 repeat measurements for 12 point source locations were made. Before each measurement, the x–y table was readjusted horizontally. The reproducibility of the absolute angulation error measurements, which included the error caused by readjustment, was calculated as the SD of each of the repeatedly measured angulation error values. The results were better than 0.32° (0.11° average). We performed a second series of repeat measurements without in-between readjustment of the x–y table, i.e., with a given misalignment error. These measurements determined the accuracy of measuring relative (i.e., regional) variations in channel tilt. The respective results were better than 0.02° (0.01° average). For a fanbeam collimator, the respective results were 0.31° (0.13° average) for the absolute angulation error and 0.16° (0.10° average) without misalignment error.

All parallel-hole collimators except 1 showed similar results and were considered acceptable for SPECT imaging. An example surface map for the low-energy, general-purpose (LEGP) collimator GC is shown in Figure 6A. For all parallel-hole collimators, we used a grid spacing of 3 cm in each direction. Figure 6B shows the surface map of a parallel-hole low-energy, all-purpose (LEAP) collimator that had been in use for 7 y and was then replaced by a new collimator because of nonoptimal image quality. Table 2 gives the numeric results for all parallel-hole collimators.

TABLE 1
Collimator Specifications

Parameter	Parallel-hole collimators			Fanbeam collimator
Model	RDC-900-A	APC-34RS-C	RDC-901-A	LEHR-FAN
Type	LEGP	LEAP	LEHR	LEHR
Manufacturer	Toshiba	Elscint	Toshiba	Picker
d* (mm)	2.36	†	1.78	1.40
t (mm)	0.22	†	0.17	0.18
b (mm)	40.0	†	40.0	27.0
f (cm)				50
UFOV (cm^2)	35 × 50	40 × 54	35 × 50	24 × 40
R_0 (mm)	~4.5	~2.4	~4.0	3.5
R_{10} (mm)	~9.5	~9.1	~7.5	8.0

*All channels had hexagonal cross sections.
†Not reported.
LEHR = low-energy, high-resolution; LEGP = low-energy, general purpose; LEAP = low-energy, all-purpose; d = diameter across the flats of hexagonal channels; t = septal thickness; b = channel length; f = focal length; UFOV = useful field of view; R_0 and R_{10} = system resolution (full width at half maximum) for a source– collimator distance of 0 and 10 cm, respectively.

Fanbeam Collimators

For the first part of the measurement we used a point source grid of 5 rows spaced 4 cm apart. The spacing within the rows was 3 cm. Figure 5 plots the image centroid coordinates averaged over all rows versus the corresponding point source locations. The linear regression coefficients of both lines almost equal 1. The accuracy of determining the position of the symmetry line was better than 0.4 mm (Table 3). For the second part of the measurement procedure, the close-distance grid spacings remained unchanged. The remote-distance grid was adapted according to Equation 3. Figure 7 shows surface maps for the fanbeam collimators RN1 and RN3. Numeric results for all fanbeam collimators are given in Table 3.

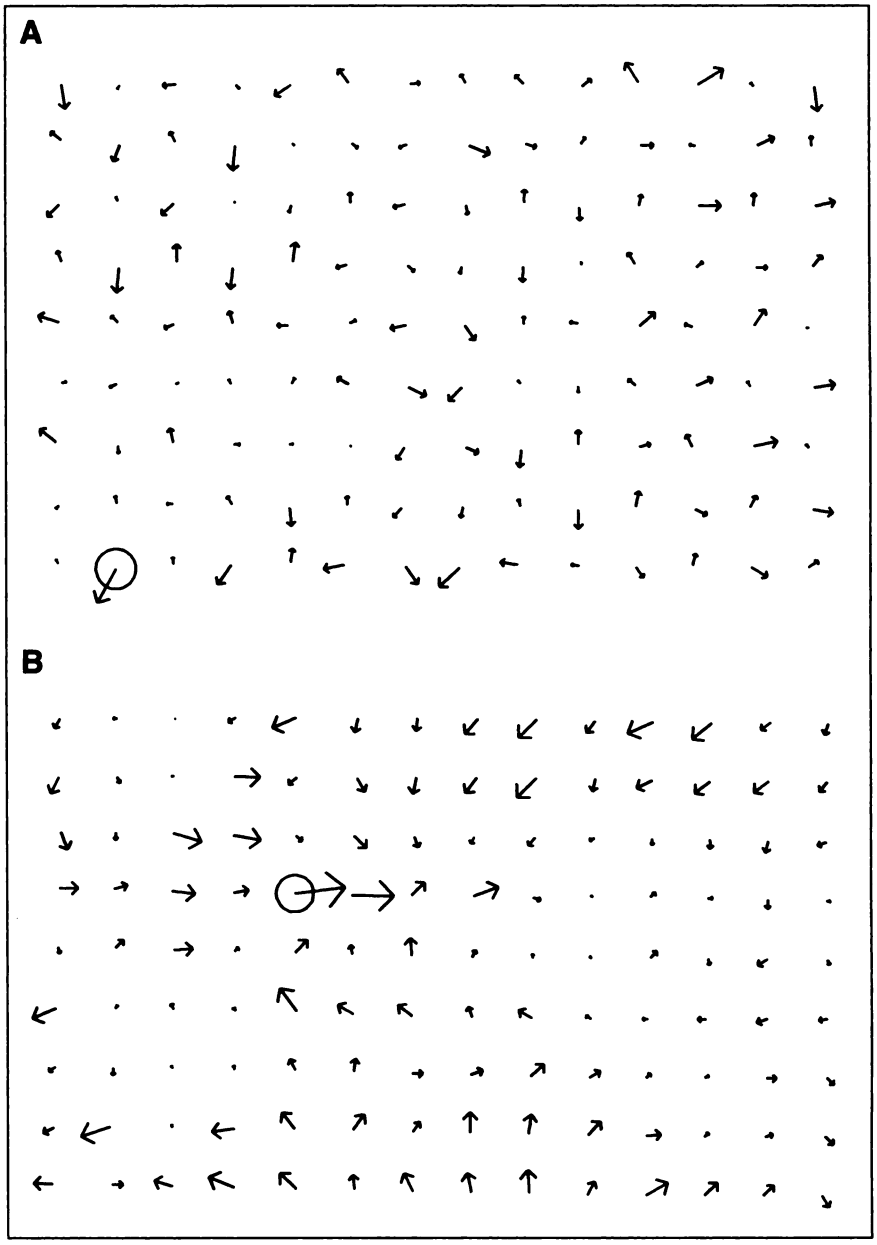

FIGURE 6. Angulation error surface maps for parallel-hole collimators GC (A) and H1 (B). Rectangle outlines useful field of view of collimator. Length and direction of each arrow indicate magnitude and direction of total angulation error α at respective measurement locations. Circles mark maximum results of 0.96° (A) and 1.36° (B), respectively. Radii represent acceptance limit of 0.5° in both cases. Axis of rotation of camera is parallel to long axis of collimators. In contrast to collimator GC, collimator H1 shows regions of strong directional uniformity.

TABLE 2
Angulation Error Results for Parallel-Hole Collimators

Type	No.	Mean	Maximum	SD
LEGP	GC	0.33°	0.96°	0.17°
	GA	0.25°	0.64°	0.12°
	RD	0.40°	1.27°	0.20°
	GE1	0.39°	1.26°	0.20°
	GE2	0.42°	1.49°	0.24°
LEAP	H1	0.38°	1.36°	0.22°
LEHR	GC	0.24°	0.76°	0.13°

Mean = mean angulation error value averaged over all measurement locations; maximum = maximum angulation error value; SD = SD of all angulation error values; LEHR-low-energy, high-resolution.

DISCUSSION

We have used the measurement principle introduced by Chang et al. (*1*) and Busemann-Sokole (*7*). Both authors used special Lucite jigs to investigate parallel-hole collimators. The recommended and widely recognized acceptance limit for angulation errors of 0.5°, proposed by Busemann-Sokole (*9*), serves as the basis of our assessments. Gantet et al. (*10*) performed a computer-simulation study on the influence of collimator defects on image uniformity. They found that an angulation error of ±0.22° results in a 1% image nonuniformity. Some collimator manufacturers guarantee a tolerance level of 0.25° (*10*). Malmin et al. (*11*) developed a highly accurate (±0.05° root-mean-squared error) industrial method of producing complete angulation error maps. Unfortunately, the large experimental and computational effort and the amount of radioactivity used render

TABLE 3
Angulation Error Results for Fanbeam Collimators

Type	No.	Mean	Maximum	SD	Center offset* (mm)	m_c/m_r*
LEHR	RN1	0.16°	0.29°	0.08°	1.0 ± 0.3	0.7996 ± 0.0018
LEHR	RN2	0.16°	0.27°	0.07°	1.1 ± 0.3	0.7967 ± 0.0005
LEHR	RN3	0.23°	0.42°	0.08°	1.3 ± 0.4	0.7976 ± 0.0003

*Given error is SD from averaging over all grid rows.

Mean = mean angulation error value averaged over all measurement locations; maximum = maximum angulation error value; SD = SD of all angulation error values; center offset = collimator center position in grid coordinates (Fig. 4); m_c/m_r = ratio of magnification factors as used in Equation 3; LEHR = low-energy, high-resolution.

this technique unfit for routine applications. Furthermore, the technique can be applied only to parallel-hole collimators. Several authors performed qualitative examinations of collimators by checking the center of rotation offset (*3,5,12–15*). An offset >0.5 pixel over a 180° camera head turn can in itself cause a noticeable loss of resolution (*3,13*).

The measurements with and without in-between readjustment of the x–y table showed that the measurement accuracy

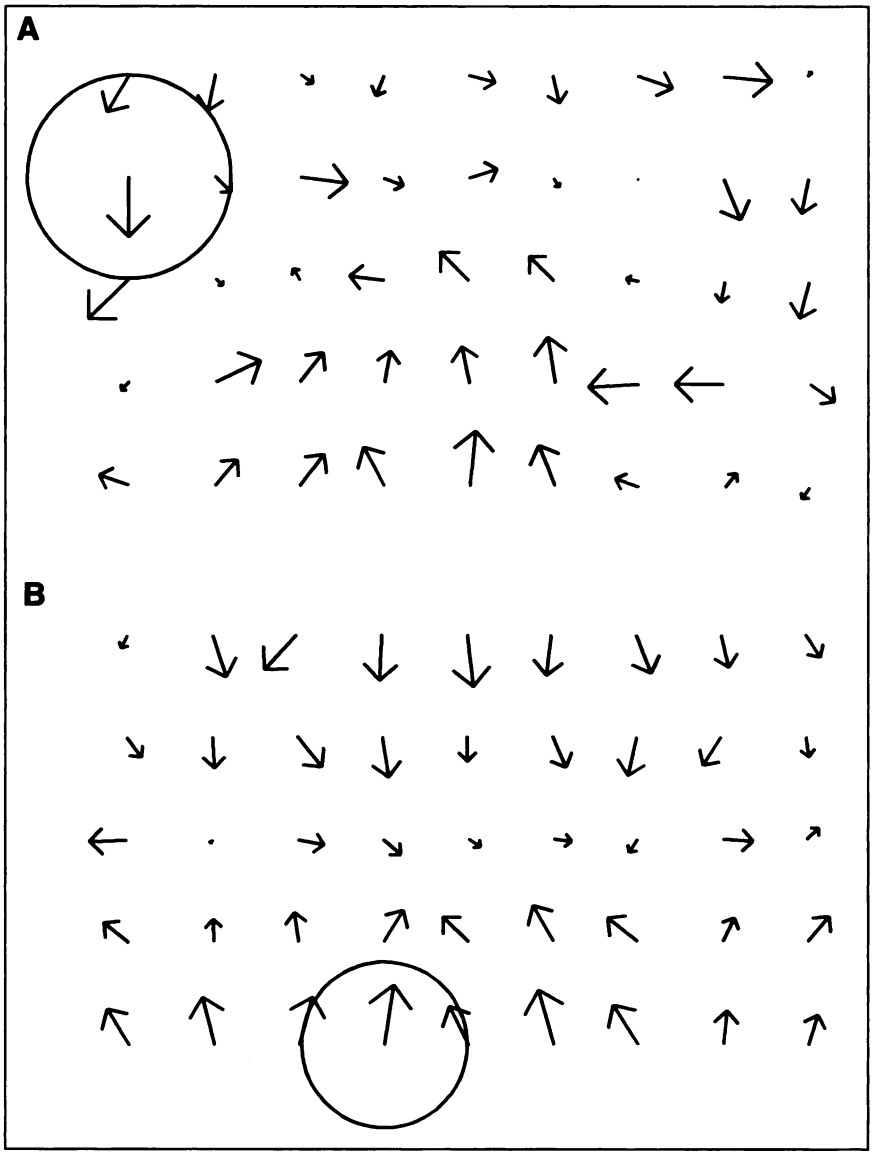

FIGURE 7. Angulation error surface maps for LEHR fanbeam collimators RN1 (A) and RN3 (B). Circle radius represents 0.5° in both cases. Maximum results marked by circle are 0.30° (A) and 0.36° (B), respectively. Axis of rotation of camera is parallel to short axis of collimator. Collimator RN1 exhibits region of directional uniformity in its lower central part. Orientation pattern of arrows in collimator RN3 is typical of concavity.

achieved by our technique under routine working conditions was limited mainly by inevitable manual misalignment. But this error simply offset each absolute angulation value by a constant amount that was smaller than 0.63° in all cases. For all surface maps presented in this article, this offset has been subtracted. Regional variations of channel tilt can still be detected with high reproducibility (better than 0.16°). The accuracy of measuring absolute angulation values is 0.32°. It is therefore well suited to examine the condition of a collimator in terms of global correct channel alignment because it is well below the acceptance limit of 0.5°. Regional variations of channel tilt, which may cause nonuniformities in an image, can be assessed with much higher precision.

All parallel-hole collimators except 1 were in good condition and acceptable for high-resolution SPECT imaging. Except for a few isolated channels, all angulation error values were below 0.5° and showed small variations in magnitude. The channels were oriented randomly across the collimator face. The surface map of the defective LEAP collimator H1 (Fig. 6B) indicated a concavity of the collimator because the arrows in its central part generally pointed toward its long center line and increased in length with increasing distance from it. This example shows that some collimator defects can be revealed only by detailed surface maps because the mean and SD angulation error values were acceptable.

Only 1 of the 3 fanbeam collimators tested was acceptable without reservations for SPECT imaging. The surface map of this collimator (Fig. 7A) showed a limited region of directional uniformity. But because the arrows outside this region were randomly oriented and because of the smallness of all angulation error values, we considered this collimator still acceptable. The 2 remaining fanbeam collimators fulfilled the numeric acceptance criteria mentioned above. However, their angulation error maps clearly exhibited directional systematics that could affect the quality of SPECT images. The surface map of collimator RN3 in Figure 7B suggested a concavity similar to the one discussed above. Collimator RN2 showed similar but less pronounced results. We note that a mismatch of the grid spacings would also have resulted in a directional trend, but with all arrows pointing toward the short axis of the collimator. A concavity in the direction of the fan might have increased the tilt of all channels in such a way as to simulate a fan with a slightly shorter convergence length. This could explain the smaller m_c/m_r values of collimator RN2 and RN3 in comparison with collimator RN1 (Table 3) and their discrepancy with the nominal value of $m_c/m_r = 0.7988$. This disagreement translates to an addition of 0.15° and 0.08° to the nominal channel tilt of 13.50° at the marginal point source locations on the long axis for collimator RN2 and RN3, respectively. Compared with the bending along the short axis, the effect is small.

The direction of the conjectural bendings suggests that they may have been caused by placing heavy objects on the collimator while it was on the exchange cart or by sagging in the storage rack from the heavy weight of the collimator. One should keep in mind that in spite of their massiveness, collimators are sensitive to mechanical influence.

All of our collimators were of the foil type and had been in use for 7 y. Unlike other authors (*1,2,4,5,10,11,16,17*), we have not found that foil collimators are generally of inferior quality. In agreement with Graham (*6*), we recommend a time interval for quality control checks of 3 mo for low-energy and of 6 mo for high-energy collimators.

All equipment was tested at our department, which is equipped with 12 γ cameras for both acceptance testing and routine quality control of collimators used for SPECT. The method was easy to implement, because the scanning hardware consists of a standard computer-controlled x–y scanning table with only the precision distance holder as an additional special part. The present implementation of the analysis software is based on a widely used numeric processing language but requires that the images be imported into the software system for analysis. We anticipate, however, that because of the low frequency of routine tests, only larger departments will fully use such equipment, whereas small departments may share the equipment or will make use of similarly equipped medical physics services for routine quality control.

CONCLUSION

This technique is suited for comprehensive measurement of collimator angulation. We have expanded the measurement principle to allow for testing not only of parallel-hole collimators but also of fanbeam, converging, and diverging collimators, regardless of their individual geometry. The measurement procedure is independent of technical collimator specifications, because relevant parameters are calculated from the measurement itself. Regional variations in channel tilt can be detected with high accuracy. This enables us to reveal subtle mechanical deformations of collimators. Numeric values alone do not fully characterize the condition of a collimator in terms of angulation error, but surface maps should be used to discover regional preferences in channel orientation. Automation of the measurement and evaluation process make this method suitable for both acceptance tests and routine quality control checks.

ACKNOWLEDGMENTS

The authors thank Walter Piller, Peter Schaffarich, and Angela Taubeck for frequent technical assistance and Alfred Gamperl for construction of mechanical components. We thank Dr. Werner Backfrieder for helping to transfer image data through the network. We especially appreciate the cooperation of Dr. Beatrix König and the staff of the Nuclear Medicine Department of the Hanusch Hospital in Vienna.

REFERENCES

1. Chang W, Li S, Williams J, et al. New methods of examining gamma camera collimators. *J Nucl Med.* 1988;29:676–683.

2. Blend MJ, Patel BA, Rubas D, Bekerman C, Byrom E. Foil collimator defects: a comparison with cast collimators. *J Nucl Med Tech.* 1992;20:18–22.
3. Farrell TJ, Cradduck TD, Chamberlain RA. The effect of collimators on the center of rotation in SPECT. *J Nucl Med.* 1984;25:632–633.
4. Chang W, Bruch P, Wesolowski C, Kirchner PT, Ehrhardt JC. Performance of cast collimators for SPECT imaging [abstract]. *J Nucl Med.* 1985;26:P44.
5. O'Connor MK. Instrument- and computer-related problems and artifacts in nuclear medicine. *Semin Nucl Med.* 1996;26:256–277.
6. Graham LS. The AAPM/RSNA physics tutorial for residents: quality control for SPECT systems. *RadioGraphics.* 1995;15:1471–1481.
7. Busemann-Sokole E. Measurement of collimator hole angulation and camera head-tilt for slant and parallel hole collimators used in SPECT. *J Nucl Med.* 1987;28:1592–1598.
8. *Performance Measurements of Scintillation Cameras.* Standards publication NU-1–1994. Washington, DC: National Electric Manufacturers Association; 1994.
9. Busemann-Sokole E. *Quality Assurance in Nuclear Medicine Imaging.* Amsterdam, The Netherlands: Rodopi; 1990.
10. Gantet P, De Lagrevol R, Danet B, De la Barre F, Guiraud R. Simulation study of the influence of collimator defects on the uniformity of scintigraphic images [in French]. *Phys Med Biol.* 1997;42:603–609.
11. Malmin RE, Stanley PC, Guth WR. Collimator angulation error and its effect on SPECT. *J Nucl Med.* 1990;31:655–659.
12. Karlovich CA, Halama JR, Henkin RE. Affects of unseen collimator defects on center of rotation measurements [abstract]. *J Nucl Med Technol.* 1990;18:137.
13. Cerqueira MD, Matsuoka D, Ritchie JL, Harp GD. The influence of collimators on SPECT center of rotation measurements: artifact generation and acceptance testing. *J Nucl Med.* 1988;29:1393–1397.
14. Yoshizumi TT, Suneja SK, Teal JS, Sutton AM, Collyer D. Defective parallel-hole collimator encountered in SPECT: a suggested approach to avoid potential problems. *J Nucl Med.* 1990;31:1892–1893.
15. O'Connor MK, Oswald WM. Influence of collimators on SPECT center of rotation measurements. *J Nucl Med.* 1989;30:265–266.
16. Yeh E. Polarity in a hexagonal collimator. *J Nucl Med.* 1983;24:1203–1204.
17. Gillen GJ. Nonisotropic point spread function as a result of collimator design and manufacturing defects. *J Nucl Med.* 1988;29:1096–1100.